Biochemical and Biophysical Research Communications 381 (2009) 70–74

Contents lists available at ScienceDirect

Biochemical and Biophysical Research Communications

journal homepage: www.elsevier.com/locate/ybbrc

CtBP1/BARS Gly172 → Glu mutant structure: Impairing NAD(H)-binding and dimerization

Marco Nardini [a], Carmen Valente [b], Stefano Ricagno [a], Alberto Luini [b], Daniela Corda [b], Martino Bolognesi [a,*]

[a] Department of Biomolecular Sciences and Biotechnology, CNR-INFM and CIMAINA, University of Milano, Via Celoria 26, I-20133 Milano, Italy
[b] Department of Cell Biology and Oncology, Consorzio Mario Negri Sud, I-66030 Santa Maria Imbaro (Chieti), Italy

ARTICLE INFO

Article history:
Received 4 February 2009
Available online 10 February 2009

Keywords:
CtBP
BARS
Transcription co-repressor
Golgi membrane fission
NAD(H)
Dimerization

ABSTRACT

C-terminal binding proteins (CtBPs) are multi-functional proteins involved in nuclear transcriptional co-repression, Golgi membrane fission, and synaptic ribbon formation. Binding of NAD(H) to CtBPs promotes dimerization. CtBP dimers act as a scaffold for multimeric protein complex formation, thus bridging transcriptional repressors and their targets in the nucleus. Based on size-exclusion chromatography experiments and on the crystal structure of the NAD(H)-free G172E CtBP mutant, we show here that absence of NAD(H) induces flexibility/backbone conformational changes at the dimerization interface and at the CtBP interdomain region. The results presented shed first light on the correlation between NAD(H)-binding and functional CtBP dimerization.

The C-terminal binding proteins (CtBPs), hosting CtBP1, CtBP1-S (or short-CtBP1, also known as CtBP1/BARS, where BARS is the acronym for Brefeldin A-ADP Ribosylated Substrate), and CtBP2 isoforms, are multi-functional proteins implicated in gene regulation, Golgi maintenance and synaptic ribbon formation [1–3]. More than thirty different transcription factors have been reported to recruit CtBPs to mediate transcriptional repression of various target genes. Most of these factors interact with CtBPs through binding motifs that closely resemble the adenovirus E1A CtBP-binding motif PLDLS [4,5], as well as through a second redundant motif known as the RRT motif [6]. In the nucleus CtBPs build the structural core of a MDa repressor complex containing sequence-specific DNA-binding repressors, enzymes such as histone deacetylases, histone lysine methyl transferases and a histone lysine-specific demethylase, and several co-repressors [7]. Interestingly, the CtBPs have been reported to be dual-function proteins, active also in the cytosol as components of a membrane fissioning machinery operating at different intracellular membrane traffic steps [2,8]. The control of CtBP nuclear vs cytosolic localization involves post-translational modifications such as phosphorylation and sumoylation [9,10].

Although the precise way CtBP recruits its partner proteins in the nucleus is not yet known, a key role is ascribed to the ability of CtBP to associate into dimers, whose association mode has been elucidated through crystal structure analyses (CtBP1, CtBP1/BARS, and CtBP2 isoforms, all lacking about 80 C-terminal residues, and all in complex with NAD(H)) [11–13]. CtBP is composed of three domains: (i) the substrate-binding domain, primarily comprising the PXDLS-binding cleft (*X* = any residue); (ii) the central nucleotide-binding domain, responsible for NAD(H)-binding and for dimerization, hosting the RRT-binding motif; and (iii) an intrinsically unstructured C-terminal region [6,11–13]. Association through two nucleotide-binding domains builds the central core of the dimer, with substrate-binding and the C-terminal domains of each monomer at opposite poles of the assembled dimer [12,13]. The CtBP nucleotide-binding domain hosts a Rossmann fold, similar to D-2-hydroxyacid dehydrogenases, including the typical G/AxGxxG(17x)D NAD-binding consensus motif, and a putative dehydrogenase active site containing a conserved His-Glu-Arg catalytic triad [11,12]. While the NAD^+-dependent dehydrogenase activity of CtBP has been demonstrated only marginally [11], consensus has emerged on the role of NAD^+/NADH-binding as the structural requirement leading to a stable dimer that would act as an aggregation scaffold for multimeric nuclear protein complexes [14]. Indeed, while possibly not fully preventing formation of the CtBP dimeric species, loss of NAD^+/NADH-binding induced a dramatic decline in homodimerization efficiency and transcriptional repression activity both in CtBP1 and CtBP2 isoforms [15,16].

Abbreviations: CtBP, C-terminal binding protein; BARS, brefeldin A-ADP ribosylated substrate; t-CtBP1/BARS, truncated-CtBP1/BARS; wt, wild-type; rmsd, root mean squared deviation; CoA, coenzyme A.

* Corresponding author. Fax: +39 02 50314895.
E-mail address: martino.bolognesi@unimi.it (M. Bolognesi).

0006-291X/$ - see front matter © 2009 Elsevier Inc. All rights reserved.
doi:10.1016/j.bbrc.2009.02.010

In the present communication we show a correlation between NAD(H)-binding and CtBP dimerization, based on size-exclusion chromatography experiments, and we shed first light on the structural regions involved in the dimer-monomer transition by X-ray crystallographic analysis of the NAD(H)-free Gly172 → Glu (G172E) mutant of a truncated form of CtBP1/BARS (t-CtBP1/BARS, devoid of 80 C-terminal residues).

Materials and methods

Protein expression and purification. His-tagged t-CtBP1/BARS (1–350 aa) was expressed as described previously [12], while the His-tagged t-CtBP1/BARS G172E mutant was generated from the pET11d-His-t-CtBP1/BARS plasmid using the QuikChange Site-Directed Mutagenesis Kit (Stratagene), with the following oligonucleotide (only forward primer indicated) 5′-CATCATTGGACTAGAGCGTG TGGGCCAGG-3′. Both of these proteins were purified as previously described for the gel filtration analysis [17] or for the crystallization conditions [12].

Size-exclusion chromatography. Five milligram (at about 2.2 mg/ml) of purified t-CtBP1/BARS wild-type protein (t-CtBP1/BARS wt) and t-CtBP1/BARS G172E mutant were dialyzed in PBS buffer and applied to a Sephacryl S-200 High Resolution HiPrep 16/60 (Amersham Pharmacia) gel filtration column equilibrated in PBS buffer. Fractions of 1 ml were collected using an AKTA FPLC system, applying a flow rate of 0.3 ml/min PBS at 4 °C (Amersham Pharmacia). The eluted protein was detected by monitoring absorbance at 280 nm. Four mg of molecular weight standards were used: horse myoglobin (17 kDa), chicken ovalbumin (44 kDa), bovine γ-globulin (158 kDa), and bovine thyroglobulin (670 kDa), purchased from BioRad.

Crystallization, data collection and refinement. Crystallization of the purified t-CtBP1/BARS G172E mutant was attempted using the hanging-drop vapor diffusion setup. The protein solution, at 10 mg/ml concentration was equilibrated against 500 µl of precipitant solution from Crystal Screen I and II (Hampton Research, http://hamptonresearch.com) and from Wizard I and II (Emerald BioSystems, http://www.jenabioscience.com), at 4 and 21 °C. No crystal suitable for X-ray data collection could be grown in any of the tested crystallization conditions.

Alternatively, single crystals of the G172E mutant could be grown by using the cross-seeding technique [18]. Cross-seeding crystallization experiments were performed using the hanging-drop vapor diffusion setup by streak-seeding a single crystal of a NAD(H)-bound t-CtBP1/BARS wt on crystallization droplets containing the NAD(H)-free G172E mutant sample. The G172E protein concentration (10 mg/ml) and the crystallization solutions were identical to those used for the crystallization of NAD(H)-bound t-CtBP1/BARS wt (1.8–2.1 M ammonium formate, 0.1 M HEPES, pH 7.5) [12]. Cross-seeded crystals grew in a few days. They were then used to seed one subsequent series of experiments, thus "diluting out" the effect of the heterogeneous seeds. Such crystal "diluting" procedure was carried out twice.

The G172E crystals belong to the space group $P6_422$, with unit cell parameters: $a = b = 89.2$ Å, $c = 160.3$ Å, one molecule per asymmetric unit. A full diffraction data set was collected at 3.4 Å resolution using synchrotron radiation (ID14-EH3 beamline, ESRF, Grenoble, France). All diffraction data were processed using DENZO and SCALEPACK [19]. The structure of the G172E mutant was determined by molecular replacement methods using the program MolRep [20]. The crystal structure of NAD(H)-bound t-CtBP1/BARS (PDB entry-code 1HKU) [12] was used as search model, after deleting the atomic coordinates for NAD(H). The structure was then refined using the program REFMAC [21] (rigid body, restrained refinement, isotropic B-factor refinement). Model building and structure analysis was performed with COOT [22]. The program PROCHECK [23] was used to assess the stereochemical quality of the protein structure. Coordinates and structure factors have been deposited with the Protein Data Bank with accession codes 3GA0 and r3GA0sf, respectively.

Results

Gel filtration analysis of the role of NAD(H)-binding in CtBP1/BARS homodimerization

To investigate the role of NAD(H)-binding in the formation of the t-CtBP1/BARS homodimer, we generated a t-CtBP1/BARS mutant, where residue Gly172 in the NAD(H)-binding site is replaced with Glu (t-CtBP1/BARS G172E), thus preventing the binding of NAD(H), as previously demonstrated for the full-length G172E protein [12]. The oligomerization state of t-CtBP1/BARS wt was compared with that of the G172E mutant by gel filtration using a Sephacryl S-200 16/60 GF column. Fig. 1 shows the elution patterns of both the t-CtBP1/BARS G172E mutant and wt proteins. The elution volumes on a calibrated Sephacryl S-200 16/60 column were used to calculate the molecular mass of each protein.

We previously reported the crystal structure of t-CtBP1/BARS in a binary complex with NAD(H) [12] in which each monomer had a molecular mass of 39 kDa. As shown in Fig. 1B, for t-CtBP1/BARS, the major peak eluted at 50.73 ml. This peak corresponds to the expected dimeric species of t-CtBP1/BARS, with a molecular mass of about 79 kDa. A significant change in the elution pattern was seen for the t-CtBP1/BARS G172E mutant that does not bind NAD(H). Indeed, the G172E mutation resulted in complete disruption of the dimer, with a single major peak at 58.76 ml corresponding to a monomeric molecular mass of about 40 kDa (Fig. 1B).

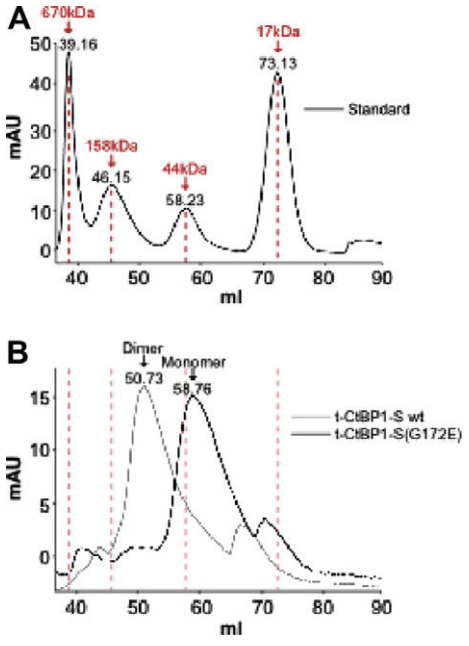

Fig. 1. (A) Size-exclusion chromatography profile for molecular weight standards. 4 mg of molecular weight standards were passed through a Sephacryl S-200 column; both molecular mass (red) and retention time (black) are indicated for each. (B) Size-exclusion chromatography profiles of wild-type t-CtBP1/BARS (residues 1–350, grey) and the t-CtBP1/BARS G172E mutant (black). 5 mg of each protein were applied to the Sephacryl S-200 column, with PBS elution at 0.3 ml/min at 4 °C. The elution patterns were detected by monitoring the absorbance at 280 nm. (For interpretation of the references to color in this figure legend, the reader is referred to the web version of this paper.)

Table 1
Data collection and refinement statistics.

Space group	$P6_422$
Resolution (Å)	29.8–3.4
Unit cell dimensions (Å)	a = 89.20, b = 89.20, c = 160.26, β = 120°
Completeness (%)	99.5 (98.9)[a]
<I/σ (I)>	8.7 (3.1)
Average multiplicity	4.4
R-factor (%)/R-free (%)[b]	26.3/33.4
No. protein atoms	2609 (residues 10–346)
No. solvent molecules	1
No. ions modeled as formate	2
rms Deviation from ideality:	
bond lengths (Å)	0.008
bond angles (°)	1.142
Average B value for main-chains (Å^2)	58.2
Average B value for side-chains (Å^2)	58.6
Average B value for all atoms (Å^2)	58.4
Ramachandran plot[c]: residues in	
most-favored and allowed regions (%)	85.0
additional allowed regions (%)	14.0
generously allowed regions (%)	1.0

[a] Values in parentheses are for the outer resolution shell 3.5–3.4 Å.
[b] R-factor = $\sum_h \| F_h^{obs} \| - \| F_h^{calc} \| / \sum_h \| F_h^{obs} \|$; R-free calculated by omitting 5% of the diffraction data.
[c] Data produced using the program PROCHECK [23].

Crystal structure of NAD(H)-free t-CtBP1/BARS G172E mutant

The structure of the t-CtBP1/BARS G172E mutant was solved and refined at 3.4 Å resolution, with R-factor and R-free values of 26.3% and 33.4%, respectively (Table 1). The overall G172E structure matches closely that of t-CtBP1/BARS wt (PDB entry 1HKU) [12] (Fig. 2A). It consists of two compact α/β Rossmann domains referred to as the nucleotide-binding (residues 1–112, 309–350) and the substrate-binding (residues 113–308) domains, respectively. The two domains are separated by a deep cleft, building the dinucleotide-binding site. The cleft hosts the typical G/AxGxxG(17x)D consensus motif for NAD(H)-binding, located in the Gly170-Asp193 stretch (Fig. 2B). In the G172E mutant, the Glu172 side-chain protrudes inside the dinucleotide-binding site, at the site hosting the NAD(H) ribose ring in the NAD(H)-bound t-CtBP1/BARS wt protein (Fig. 2B). As a result, the interdomain cleft is not occupied by the dinucleotide in the G172E mutant structure. Two electron density peaks compatible with solvent molecules have been assigned to two formate anions (from the crystallization medium) according to what had previously been found in the t-CtBP1/BARS-NAD(H) complex [12]. The absence of the bound nucleotide triggers changes in the side-chain conformation of residues Arg173, Arg255, Glu284, and His304, in the NAD(H)-binding cleft. In particular, despite the low resolution of the diffraction data, it is evident that the salt bridge between His304 ND1 and Glu284 OE1 atoms, found in the NAD(H)-bound wt structure, is not present in the NAD(H)-free mutant structure, where the Glu284 side-chain points outside of the NAD(H)-binding cleft.

The overall tertiary structure of the NAD(H)-free G172E mutant is mostly unaffected by the mutation when compared to the NAD(H)-bound t-CtBP1/BARS wt structure, the rms deviation being 0.50 Å for 331 C_α atom pairs (residues 15–345). However, specific differences on the backbone structure can be localized at the β2–α2 loop (residues 46–48, rmsd = 1.04 Å), at the αB–αC loop (residues 140–146, rmsd = 0.94 Å), at the βA–αD loop (residues 172–173, rmsd = 0.93 Å), at the αE region (residues 195–206, rmsd = 0.76 Å), at the βD–αG loop (residues 229–231, rmsd = 1.10 Å), and at the βF region (residues 281–288 and 294–297, rmsd = 1.37 Å and rmsd = 0.76 Å, respectively) (Fig. 2A). Secondary structure in the G172E mutant has been assigned accordingly to the t-CtBP1/BARS wt structure [12].

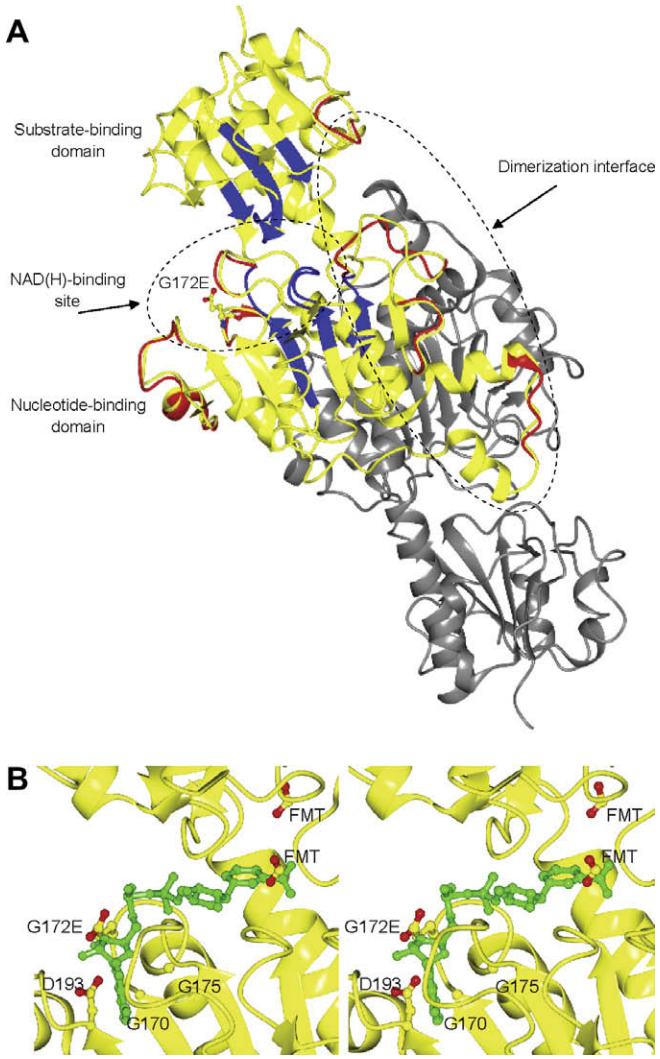

Fig. 2. (A) Dimeric structure of the NAD(H)-free G172E mutant (subunit A in yellow and subunit B in grey). The NAD(H)-bound t-CtBP1/BARS wt protein structure (red) is superimposed to the NAD(H)-free G172E mutant subunit A. Regions of the NAD(H)-free G172E mutant whose B-factors are higher than the wt NAD(H)-bound t-CtBP1/BARS are shown in blue for subunit A. The substrate- and the nucleotide-binding domains, the G172E mutation site, the dimerization interface and the NAD(H)-binding site are labeled. (B) Stereo view of the NAD(H)-binding site in the NAD(H)-free G172E mutant (yellow). The bound NAD(H) molecule in the corresponding t-CtBP1/BARS wt protein (PDB entry-code 1HKU) is shown in green. The position of the GxGxxG(17x)D NAD-binding consensus motif is indicated, with the G172E mutation highlighted. Formate ions, from the mutant protein structure, are labeled FMT. (For interpretation of the references to color in this figure legend, the reader is referred to the web version of this paper.)

Quaternary structure

The NAD(H)-free G172E mutant forms an elongated homodimer in the crystal, which is structurally equivalent to that found fort-CtBP1/BARS wt [12]. This finding was expected since a NAD(H)-bound t-CtBP1/BARS wt crystal was used to cross-seed the NAD(H)-free G172E sample. The dimer displays a two-fold crystallographic symmetry, with the central core made by pairing of two nucleotide-binding domains, whereas the two substrate-binding domains are at opposite poles of the assembled dimer (Fig. 2A). A mainly hydrophobic region builds the dimer association interface, covering 2895 Å^2 on each monomer, about 200 Å^2 smaller than the corresponding dimeric interface in the t-CtBP/BARS wt (3098 Å^2). The dimer-packing interactions are

based on contacts along the β3–α3 loop (residues 65–66) and along the β5–α5 loop (residues 112–116), on antiparallel pairing of the αA helices (residues 119–130) in the two subunits, on swapping of the αB-loop–αC motif (residues 135–162), on contacts along the βF–βG loop (residues 285–286), and on the βG–α5 region (residues 299–317) (Fig. 2A). It is worth noting that some regions at the dimeric interface (residues 140–146, residues 281–288 and 294–297, respectively, see above) are affected by structural changes relative to the dimeric NAD(H)-bound wt structure.

B-factors analysis

The average backbone B-factor (B_{ave}) for the NAD(H)-free G172E mutant is 58.4 Å^2, about 20% higher than the corresponding value of the NAD(H)-bound t-CtBP1/BARS wt (B_{ave} = 48.5 Å^2). This difference, in keeping with the lower resolution of the diffraction data from G172E crystals relative to the wt crystals (3.4 vs 2.1 Å), is however not uniformly distributed along the protein structure (Fig. 2A). Considering the difference in resolution, a meaningful B-factor comparison between NAD(H)-free G172E mutant and the NAD(H)-bound wt t-CtBP1/BARS can only be achieved if normalized backbone B-factors (for each j residue: $B_{N,j} = B_j/B_{ave}$) are considered. As a result, positive difference peaks $\Delta B_{N,j} = [(B_{N,j})_{mut}-(B_{N,j})_{wt}]/(B_{N,j})_{wt}$ can be identified at specific sites of the G172E mutant. The backbone regions of the G172E mutant that display higher average mobility than the wt protein are localized at the β1 strand (B_{17-22} = 70.1 Å^2, $\Delta B_{N,17-22}$ = 27.6%, B and ΔB_N averaged over the residue range 17–22), at the β3 strand (B_{61-65} = 62.3 Å^2, $\Delta B_{N,61-65}$ = 15.0%), at the β4 strand (B_{83-93} = 62.6 Å^2, $\Delta B_{N,83-93}$ = 16.6%), at the β5 strand ($B_{107-109}$ = 54.1 Å^2, $\Delta B_{N,107-109}$ = 18.2%), at the βA–αD region ($B_{170-174}$ = 46.9 Å^2, $\Delta B_{N,170-174}$ = 21.6%), at the βD strand ($B_{219-227}$ = 55.2 Å^2, $\Delta B_{N,219-227}$ = 24.1%), at the βD–αG region ($B_{235-236}$ = 58.1 Å^2, $\Delta B_{N,235-236}$ = 17.9%), at the βE–αH region ($B_{251-259}$ = 56.8 Å^2, $\Delta B_{N,251-259}$ = 22.5%), at the strand βF ($B_{275-281}$ = 63.3 Å^2, $\Delta B_{N,275-281}$ =31.2%), and at the βG–α5 region ($B_{302-309}$ = 49.6 Å^2, $\Delta B_{N,302-309}$ = 24.8%) (Fig. 2A).

Discussion

In recent years many reports have demonstrated that CtBPs bind NAD(H), and that dinucleotide-binding affects the overall structure of the protein, its affinity for E1A, and its transcriptional functional capability [24]. The hypothesis that NAD(H)-binding affects CtBP activity indirectly, through control of CtBP oligomerization, has gained increasing consensus [14–16]. We and others have shown that NAD(H)-binding promotes the stabilization of a compact dimeric form of the protein, with the substrate- and nucleotide-binding domains tightly wrapped around the bound NAD(H) [11,12], required for providing a stable core for the formation of a multimeric repression complex [7,14]. Mutation of the NAD(H)-binding motif (G183A/G186A) in CtBP1 leads to a protein deficient in dimerization but still with a detectable, *albeit* lower than wt, repressional activity [15]. Similarly, the amino acid substitution at G189, in the conserved NAD(H)-binding motif, abrogates the ability of CtBP2 to homodimerize, being also associated with a dramatic loss of co-repressor activity [16]. More recently, CtBP expressed in *Drosophila* showed that a NAD^+-binding mutant lacks biological activity [25]. Furthermore, the NAD(H)-binding can be competed by AcylCoAs. AcylCoAs bind to the NAD(H)-binding site and favor (i) a monomeric conformation of the protein, (ii) its cytosolic localization, and (iii) the membrane fissioning activity of the protein complex that includes the CtBP1/BARS [2,12].

While all the above data clearly indicated that the effect of NAD(H) on the transcriptional activity of CtBP is indirect, through dimerization [15,26], so far no structural details have been reported on the mechanism of dimer destabilization in the apo-protein. In this paper we showed by gel filtration experiments that t-CtBP1/BARS wt is a dimer in the presence of NAD(H). Because the protein uploads the dinucleotide during the expression procedure [12], we analyzed the structure and the oligomerization state of the ligand-free protein by using a t-CtBP1/BARS single mutant at the nucleotide-binding site (G172E). The G172E mutation affects the typical G/AxGxxG(17x)D consensus motif in the CtBP nucleotide-binding domain (Gly170-Asp193, in CtBP1/BARS), and sterically impedes NAD(H)-binding (Fig. 2B). The NAD(H)-free G172E mutant elutes in gel filtration unequivocally as a monomer (Fig. 1B).

To shed first light on the structural regions involved in the monomer-dimer transition triggered by NAD(H)-binding, we analyzed the crystal structure of the NAD(H)-free G172E mutant, and compared it to the NAD(H)-bound wt protein. At first, any attempt to crystallize the NAD(H)-free mutant failed, possibly because the absence of the bound cofactor in the NAD(H)-binding site leaves the substrate- and the dinucleotide-binding domains free to assume different relative orientations, thus preventing crystallization. We, therefore, applied a multi-stage cross-seeding crystallization technique [18], using as seeds micro-crystals of the wt NAD(H)-bound t-CtBP1/BARS [12]. This technique allowed us to grow NAD(H)-free G172E mutant crystals isomorphous with those of wt NAD(H)-bound t-CtBP1/BARS, thus selecting through crystallization the NAD(H)-free G172E molecules displaying a compact conformation similar to that adopted by the wt protein in NAD(H)-binding. In this crystal form the NAD(H)-free G172E mutant is "forced" to mimic the NAD(H)-bound wt dimer [12] (Fig. 2A); nevertheless the absence of the bound dinucleotide induces alterations in the backbone of the G172E mutant structure localized mostly at the dimerization interface and at the interdomain region. In the mutant NAD(H)-free structure, the absence of the salt bridge between His304 and Glu284 triggers a different backbone conformation in the βF region (residues 281–288), which is at the dimeric interface and faces the αB–αC region (residues 140–146) of the opposing subunit. As a consequence, the backbone of the αB–αC region (in the facing subunit) adopts a different conformation relative to the NAD(H)-bound wt structure, and loses the polar intermolecular interaction between Gln146 side-chain and the Gln46 side-chain of the first subunit. Overall these variations result in a smaller dimeric interface (loss of 200 Å^2) relative to CtBP/BARS wt protein (Fig. 2A). Furthermore, the normalized B-factor distribution reveals that the absence of the NAD(H) molecule in the dinucleotide-binding site has an influence on the flexibility of the protein region at the interdomain interface, in particular at the β3 strand (residues 61–65), at the βF strand (residues 275–281), and at the βG–α5 region (residues 302–309) (Fig. 2A). Based on these structural evidences, we conclude that the absence of the bound nucleotide translates into backbone conformational changes at the dimerization interface coupled to an increased flexibility at the interdomain regions. These effects, likely triggered by loss of the His304—Glu284 salt bridge in the NAD(H)-free nucleotide-binding pocket, could be observed despite the fact that the crystal growth techniques, thus the crystal lattice packing, forced the NAD(H)-free G172E mutant to dimerize. Therefore, they are expected to take place on a broader scale when the apo-CtBP protein is in solution, being sufficient to shift the association equilibria towards the monomeric CtBP species, as shown by the gel filtration analyses (Fig. 1B). It is worth noting that such a conformational variations at the dimeric interface have never been reported for any other CtBP1 or CtBP2 NAD(H)-bound structure, and therefore they seem to be related only to the absence of the bound nucleotide.

Acknowledgments

We thank Claudia Cericola (Mario Negri Sud) for excellent technical assistance. This work was supported by the Italian Ministry of Education, University and Research (PRIN project No. 2006054004_001 to MB), by the Italian Association for Cancer Research (AIRC, Milan, Italy) and Telethon (Italy); C.V. received a fellowship from the Italian Foundation for Cancer Research (FIRC, Milan, Italy).

References

[1] G. Chinnadurai, CtBP, an unconventional transcriptional corepressor in development and oncogenesis, Mol. Cell 9 (2002) 213–224.
[2] D. Corda, A. Colanzi, A. Luini, The multiple activities of CtBP/BARS proteins: the Golgi view, Trends Cell. Biol. 16 (2006) 167–173.
[3] S. Tom Dieck, F. Schmitz, J.H. Brandstatter, CtBPs as synaptic proteins, in: G. Chinnadurai (Ed.), CtBP Family Proteins, Landes Biosciences, Georgetown, Texas, USA 2005. Available from: <http://eurekah.com/abstract.php?chapid=2646&bookid=198&catid=30>.
[4] U. Schaeper, J.M. Boyd, S. Verma, E. Uhlmann, T. Subramanian, G. Chinnadurai, Molecular cloning and characterization of a cellular phosphoprotein that interacts with a conserved C-terminal domain of adenovirus E1A involved in negative modulation of oncogenic transformation, Proc. Natl. Acad. Sci. USA 92 (1995) 10467–10471.
[5] K.G.R. Quinlan, A. Verger, S.H. Kwok, J. Lee, M. Perdomo, M. Nardini, M. Bolognesi, M. Crossley, Role of the C-terminal binding protein PXDLS motif binding cleft in protein interactions and transcriptional repression, Mol. Cell. Biol. 26 (2006) 8202–8213.
[6] K.G.R. Quinlan, M. Nardini, A. Verger, P. Francescato, P. Yaswen, D. Corda, M. Bolognesi, M. Crossley, Specific recognition of ZNF217 and other zinc finger proteins at a surface groove of C-terminal binding proteins, Mol. Cell. Biol. 26 (2006) 8159–8172.
[7] Y. Shi, J. Sawada, G. Sui, B. Affarel, J.R. Whetstine, F. Lan, H. Ogawa, M.P. Luke, Y. Nakatani, Coordinated histone modifications mediated by a CtBP co-repressor complex, Nature 422 (2003) 735–738.
[8] C. Hidalgo Carcedo, M. Bonazzi, S. Spanò, G. Turacchio, A. Colanzi, A. Luini, D. Corda, Golgi fragmentation during mitosis requires the membrane fissioning protein CtBP3/BARS, Science 305 (2004) 93–96.
[9] C.J. Barnes, R.K. Vadlamudi, S.K. Mishra, R.H. Jacobson, F. Li, R. Kumar, Functional inactivation of a transcriptional corepressor by a signaling kinase, Nat. Struct. Biol. 10 (2003) 622–628.
[10] X. Lin, B. Sun, M. Liang, Y.-Y. Liang, A. Gast, J. Hildebrand, F.C. Brunicardi, F. Melchior, X.-H. Feng, Opposed regulation of corepressor CtBP by sumoylation and PDZ binding, Mol. Cell 11 (2003) 1389–1396.
[11] V. Kumar, J.E. Carlson, K.A. Ohgi, T.A. Edwards, D.W. Rose, C.R. Escalante, M.G. Rosenfeld, A.K. Aggarwal, Transcription corepressor CtBP is a NAD^+-regulated dehydrogenase, Mol. Cell 10 (2002) 857–869.
[12] M. Nardini, S. Spanò, C. Cericola, A. Pesce, A. Massaro, E. Millo, A. Luini, D. Corda, M. Bolognesi, CtBP/BARS: a dual-function protein involved in transcription co-repression and golgi membrane fission, EMBO J. 22 (2003) 3122–3130.
[13] M. Nardini, D. Svergun, P.V. Konarev, S. Spanò, M. Fasano, C. Bracco, A. Pesce, A. Donadini, C. Cericola, F. Secundo, A. Luini, D. Corda, M. Bolognesi, The C-terminal domain of the transcriptional co-repressor CtBP is intrinsically unstructured, Protein Sci. 15 (2006) 1042–1050.
[14] J. Turner, M. Crossley, The CtBP family: enigmatic and enzymatic transcriptional co-repressors, Bioessays 23 (2001) 683–690.
[15] M. Kuppuswamy, S. Vijayalingam, L.-J. Zhao, Y. Zhou, T. Subramanian, J. Ryerse, G. Chinnadurai, Role of the PLDLS-binding cleft region of CtBP1 in recruitment of core and auxiliary components of the corepressor complex, Mol. Cell. Biol. 28 (2008) 269–281.
[16] S.S.C. Thio, J.V. Bonventre, S. I-Hong Hsu, The CtBP2 co-repressor is regulated by NADH-dependent dimerization and possesses a novel N-terminal repression domain, Nucleic Acids Res. 32 (2004) 1836–1847.
[17] C. Valente, S. Spanò, A. Luini, D. Corda, Purification and functional properties of the membrane fissioning protein CtBP/BARS, Methods Enzymol. 404 (2005) 296–316.
[18] E.A. Stura, I.A. Wilson, Analytical and production seeding techniques, Methods 1 (1990) 38–49.
[19] Z. Otwinoski, W. Minor, Processing of X-ray diffraction data collected in oscillation mode, Methods Enzymol. 276 (1997) 307–326.
[20] A. Vagin, A. Teplyakov, MOLREP: an automated program for molecular replacement, J. Appl. Crystallogr. 30 (1997) 1022–1025.
[21] G.N. Murshudov, A.A. Vagin, E.J. Dodson, Refinement of macromolecular structures by the maximum-likelihood method, Acta Crystallogr. D Biol. Crystallogr. 53 (1997) 240–255.
[22] P. Emsley, K. Cowtan, Coot: model-building tools for molecular graphics, Acta Crystallogr. D Biol. Crystallogr. 60 (2004) 2126–2132.
[23] R.A. Laskowski, M.W. MacArthur, D.S. Moss, J.M. Thornton, PROCHECK, a program to check the stereochemical quality of protein structures, J. Appl. Crystallogr. 26 (1993) 283–291.
[24] P. Balasubramanian, L.-J. Zhao, G. Chinnadurai, Nicotinamide adenine dinucleotide stimulates oligomerization, interaction with adenovirus E1A and an intrinsic dehydrogenase activity of CtBP, FEBS Lett. 537 (2003) 157–160.
[25] P. Mani-Telanga, M. Sutrias-Grau, G. Williams, D.N. Arnosti, Role of NAD binding and catalytic residues in the C-terminal binding protein corepressor, FEBS Lett. 581 (2007) 5241–5246.
[26] A. Verger, K.G.R. Quinlan, L.A. Crofts, S. Spanò, D. Corda, E.P. Kable, F. Braet, M. Crossley, Mechanisms directing the nuclear localization of the CtBP family proteins, Mol. Cell. Biol. 26 (2006) 4882–4894.